Three-Dimensional Mean-Shift Edge Bundling for the Visualization of Functional Connectivity in the Brain

Joachim Böttger, Alexander Schäfer, Gabriele Lohmann, Arno Villringer, and Daniel S. Margulies

Abstract—Functional connectivity, a flourishing new area of research in human neuroscience, carries a substantial challenge for visualization: while the end points of connectivity are known, the precise path between them is not. Although a large body of work already exists on the visualization of anatomical connectivity, the functional counterpart lacks similar development. To optimize the clarity of whole-brain and complex connectivity patterns in three-dimensional brain space, we develop mean-shift edge bundling, which reveals the multitude of connections as derived from correlations in the brain activity of cortical regions.

Index Terms—Visualization applications, information visualization, visualization techniques and methodologies

◆

1 INTRODUCTION

A core challenge in understanding brain organization is the visualization of its connectivity. Sophisticated visualizations of anatomical tracts based in diffusion-weighted imaging (DWI) have proven essential to elevating the methodology. However, *functional connectivity*, an emerging approach based in the correlations of spontaneous brain activity, lacks effective visualization methods to clarify the inherent complexity of the connectivity graph.

Visualization of connectivity has almost exclusively focused on depicting spatially constrained anatomical tracts. However, *functional connectivity* [1] presents a novel problem for visualization. Functional connectivity is based on the statistically determined similarity between time-courses of activity in different brain areas. Since the first description of this method using data acquired "at rest" in 1995 [2], it has grown into a flourishing field of research (for a review, see [3]). Although functional connectivity represents connections between brain regions, the precise anatomical path is unknown. This poses an exciting opportunity for visualization, as the representation of connections is constrained only by the optimization of visual clarity, and not the requirement to represent anatomical paths.

We describe our development of an *edge bundling* method to obtain a clearer picture of functional brain connectivity. To our knowledge, this is the first application of a visualization method to depict high-resolution functional connectivity data across functional networks in its native anatomical space. Our method does not require selection of seed regions of interest, subdivision of the data into independent components, or other data reduction steps such as spatial downsampling. Although the edge bundling algorithm we use is an adaption of previous work, it contributes a stable and straightforward implementation for brain connectivity data. In this paper, we first introduce the data, and then describe our method to visualize full graphs of functional brain connectivity in anatomical three-dimensional brain space.

2 BACKGROUND

2.1 Connectomics

The defining feature of the nervous system has long been recognized as its interconnectedness, but the tools to noninvasively map such connections have only emerged in the past decade. Notably, Francis Crick, codiscoverer of the molecular structure of DNA, lamented the dearth of knowledge about the connectivity of the human brain, and outlined an agenda for pursuing this line of research [4]. Twenty years later, this research agenda is at the forefront of the neuroscience community's current concerns, and several major initiatives have brought further support to this line of research (e.g., Human Connectome Project[1] and International Neuroimaging Data-Sharing Initiative[2]).

2.2 Types of Connectivity

Anatomical and functional connectivity are related, but also capture distinct aspects of brain organization [5]. Brain function relies on networks consisting of spatially distributed areas. Although the anatomical connections are the primary feature defining white matter, the computational units are neurons, lying in the gray matter. The latter are the basis of functional connectivity.

2.2.1 Anatomical Connectivity

The anatomical structure of white matter tracts can be noninvasively mapped using DWI. This method takes

---

- *The authors are with the Max Planck Institute for Human Cognitive and Brain Sciences, 04103, Leipzig, Germany.*
E-mail: {boettgerj, aschaefer, lohmann, villringer, margulies}@cbs.mpg.de.

Manuscript received 6 Sept. 2012; revised 3 Apr. 2013; accepted 4 Aug. 2013; published online 13 Aug. 2013.
Recommended for acceptance by R. Machiraju.
For information on obtaining reprints of this article, please send e-mail to: tvcg@computer.org, and reference IEEECS Log Number TVCG-2012-09-0187.
Digital Object Identifier no. 10.1109/TVCG.2013.114.

[1] http://www.humanconnectomeproject.org.
[2] http://fcon_1000.projects.nitrc.org.

advantage of the nonisotropic movement of water molecules, which is impeded by the myelin constituting white matter tracts.

The success of DWI-based approaches are partly attributable to advanced visualization methods, which are widely accepted and applied in research as well as in clinical settings (for a review, see [6]). The most basic methods to visualize DWI data are voxel-based coloring schemes for local measures such as fractional anisotropy, maximum diffusion, or the direction of the largest eigenvector (for example, [7]). Higher-dimensional measurements can be visualized with glyph-based approaches (for example, [8]).

Diffusion data can also be used to trace the likely paths of underlying connections between gray matter areas, resulting in *deterministic* [9], [10], [11] reconstructions of white matter tracts. The visualization of these tracts can then be clarified, for example, by using similarities between tracts to schematize and colorize bundles [12], or using nonphotorealistic rendering techniques [13]. Instead of deterministic paths, the likelihood of the existence of anatomical connections can be calculated using *probabilistic* tractography, though visualization of probablistic tracts is more challenging [14], [15], [16], [17].

2.2.2 Functional Connectivity

Functional MRI (fMRI) is traditionally used to measure task-evoked activity in gray matter. In addition to the activation of areas in response to task stimuli, fMRI data contain spontaneous fluctuations that are not attributable to task effects. Although this task-unrelated activity was long assumed to be noise, evidence now indicates that it is functionally meaningful for describing large-scale networks. Most easily acquired in the absence of task demands, "resting-state functional connectivity" uses correlations between activity fluctuations across the brain to calculate connection strengths. Brain activity is sampled in regions of three-dimensional space with sizes ranging upwards from single raw voxels (several cubic millimeters) to averaging signal over whole lobes (several cubic centimeters). The strength of functional connectivity is then calculated by correlating the different time-courses of activity.

The visualization of the resulting data is much less well developed than for anatomical connectivity. So far, the focus in the field lies on the development of a multitude of analytic methods. Local measures of functional connectivity exist, and are visualized with standardized color schemes. The standard "seed"-based method calculates the connectivity of a single selected region, which can then be visualized using standardized color scales. Interactive and explorative software using this approach exist, and allow for movement of the seed with simultaneous observation of the changing connectivity patterns [18], [19], [20], [21], but they can show only a fraction of the whole connectivity data in a single image. Showing all the available information at once is impossible due to overlapping connectivity from different seed points. There are many other sophisticated methods for the analysis of functional connectivity (for a review of analysis methods, see [22]), most of which would profit from the development of equally sophisticated visualization methods of the results in the anatomical space. One such family of analysis methods is the attempt to decompose resting-state data into distinct components, using methods such as independent component analysis or principal component analysis (ICA/PCA). These components are postulated to represent distributed functional networks, which can partially overlap. Worsley et al. [23] visualized PCA components in conjunction with thresholded connections between voxels in anatomical space. As Worsley et al. [23] note, the overlap makes ICA/PCA components ill-suited for simultaneous display of multiple components. Color-coding has been proposed to visualize the three most prominent PCA components in a data set [24]. Graph theory-based analysis has also been the basis for sophisticated visualizations of whole-brain functional connectivity (for examples, [25], [26]), where the distances between nodes reflect functional connectivity strengths. However, these graph representations sacrifice anatomical information. For the purpose of representing both connectivity graphs and underlying anatomical space, manually illustrated abstract schematics have been used (for examples, see [27, Fig. 4], or [28, Fig. 6]). Nevertheless, similar clarity has not yet been achieved for the automated rendering based on connectivity data.

Our interest lies in visualization of functional connectivity on a level that parallels its anatomical counterpart in showing the multitude of connections in a single image. We believe such visualization methods can aid in the clarification and unification of the different modalities used in brain research: the anatomical and the more abstract functional knowledge. First steps to combine these two complementary aspects have recently been undertaken, since both functional and anatomical connectivity have unique advantages: For instance, functional connectivity is more accurate for describing the precise termination areas of long-distance connectivity, while anatomical connectivity can describe the paths between those areas [5], [29], [30]. Calamante et al. [31] take advantage of the strengths of each method to visualize the functional connectivity-informed anatomical paths by combining whole-brain probabilistic tractograms with the information from single seed-based or ICA-derived functional connectivity networks. After summing the functional connectivity values along the tracts, they create renderings that show the anatomical tracts connecting the functional areas.

What sets functional connectivity apart from anatomical connectivity is that white matter tracts have not only a defined beginning and end position, but also a well-defined shape of the connections between them, while functional connectivity lacks this connection with a well-defined shape. The termination points of functional connectivity have anatomical positions, but only the strength of the connection can be assessed from the data, as there is no knowledge of the path shape. Functional connectivity can thus be expressed through a square matrix with connectivity values for each pair of termination points and their associated anatomical positions. This data should ideally be visualized, in connection with additional spatial information to indicate anatomical location.

2.3 Edge Bundling

The problem of visualizing functional connectivity is, at its most abstract, the issue of visualizing a complex graph. With

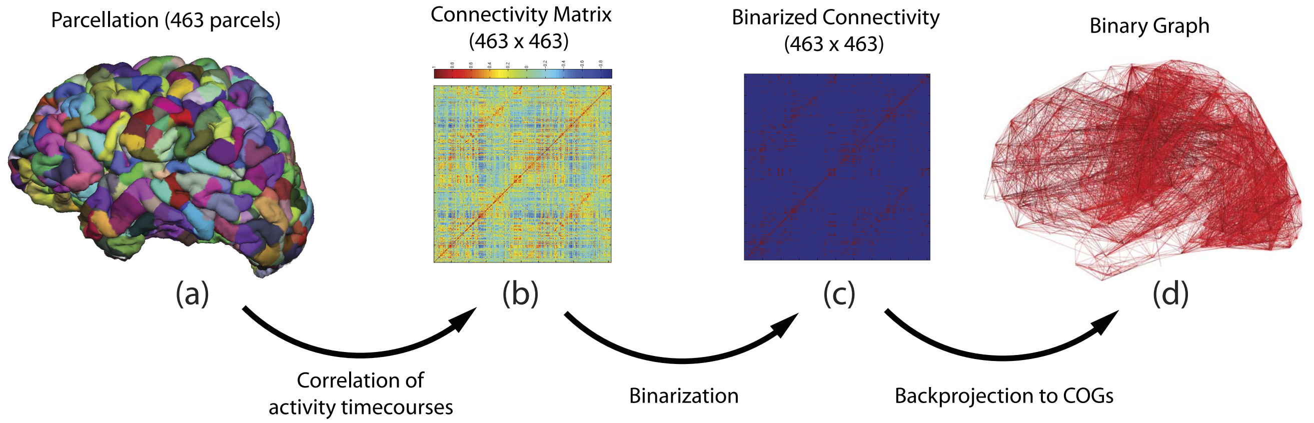

Fig. 1. Whole-brain functional connectivity data. The data that we visualize are derived from fMRI time-courses in cortical areas (a) and calculation of a correlation matrix between every pair of centers of gravity (COGs) of these regions (b). The matrix is then thresholded (c) and transformed into a binary graph. Shown is our whole-brain group-level connectivity data set; this example of connectivity between 463 cortical nodes is derived from 122 individual resting-state fMRI scans over 10 minutes each, which are then registered to a common standard coordinate system. In the unbundled graphs using straight lines (d) almost no structure is visible. We apply edge bundling to alleviate this problem.

high-resolution information, graphs of connectivity can easily contain many thousands of edges. The approach of drawing straight edges for all connections suffers from heavy clutter, and yields visualizations that resemble a ball of wool, and are not able to clearly convey the structure of the connections between different parts of the brain (Fig. 1d).

Similar visualization problems for data such as airline traffic or migration patterns have been successfully improved using *edge bundling* approaches [32], [33], [34], [35], [36], [37], [38], [39], [40]. Pioneered by Holten [32], these methods strive to change the shape of the connections visually so that related edges are grouped together, while leaving the terminal points of the connections unchanged.

The original approach, which requires a preexisting hierarchical partition of the anatomy, has recently been used for the visualization of functional connectivity [21], [33], [34]. Mapping the different parts of the brain to an abstract two-dimensional circular layout before application of the bundling algorithm has yielded beautiful visualizations of whole-brain functional connectivity. One problem with this approach, however, is assumptions necessary for creating anatomical subdivisions. Also, understanding the anatomical placement of the regions in the abstract circular layout requires the viewer to learn a new standardized brain composition.

Both abstract and anatomically faithful layouts have advantages and disadvantages depending on the context. For our main interest of high-resolution voxel-level mapping of anatomical areas on the cortex, visualization of functional connectivity in the native brain space would be advantageous. Using the anatomical space is also an advantage in the clinical setting, where pathologies may alter brain structure and make the use of standardized parcellation schemes impossible.

In contrast to methods requiring a hierarchical partition [32], [35], newer methods do not [36], [37], [38], [39], [40], [41], [42]. Holton and Wijk [36] have improved upon his original method, and presented a nonhierarchical edge bundling method for general graphs, *force-directed edge bundling (FDEB)*. This elegant method is applicable to the visualization of connectivity in the anatomical space without previous calculation of a hierarchical subdivision. However, as Hurter et al. [37] have noted, the method has several heuristically determined parameters, and relies on an unstable equilibrium between forces. Other works have addressed improvements on scalability [38], and the application to three-dimensional space [39]. However, all of these methods either require relatively complicated implementation for the required control structures [40], or possess an algorithmic element, such as sampling to image space, which makes application to three-dimensional data difficult or impossible [41], [42]. One of the latter methods is *kernel density estimation edge bundling (KDEEB)* [37], which calculates the gradient of the density of the edges in image space by summation of kernels based at the subdivision points or around the edges, and then iteratively moves subdivision points into regions with higher density.

Our approach, which is described in the next section, combines the straightforward applicability in three-dimensional space and concept of compatibility from FDEB with the numerical stability and ease of use of KDEEB.

3 MEAN-SHIFT EDGE BUNDLING FOR THE VISUALIZATION OF FUNCTIONAL CONNECTIVITY

Our approach to advance the visualization of functional connectivity is to apply edge bundling to improve its clarity in the three-dimensional anatomical brain space. Our method is strongly inspired by FDEB and KDEEB, and we present here its first application to functional connectivity.

3.1 Data

We visualize resting-state connectivity from two data sets. First, a *whole-brain data set* derived from a group of participants for an overview of large-scale connectivity. Second, a *detail data set* of the left hemisphere derived from a single participant to show the feasibility of our approach for single cases, and to show the details that are potentially lost in group-level analysis.

Both data sets consist of binary graphs with the nodes based on voxels or cortical parcels and edges between strongly connected nodes. For the whole-brain group data, 122 data sets from healthy participants between the ages of 18 and 60 were downloaded from fcon_1000.projects.nitrc.org, and preprocessed as previously described [43]. All data sets were collected by the Nathan Kline Institute and made available by the International Data Sharing Initiative [44]. Part of the preprocessing was the parcellation of the data sets into 463 cortical and subcortical parcels [45]. For each data set, a connectivity matrix was then calculated using Pearson correlation between the average time series of these parcels.

After Fisher's r-to-z transformation, the correlation values were averaged across subjects and the connections further thresholded to only leave the top 7.5 percent ($z > 0.432$). We use a binary graph because inclusion of all weighted connections would not be feasible due to current memory and computational limitations. Thresholding also has the neuroscientific advantage of excluding less significant and negative correlations, whose anatomical significance may be ambiguous [46], [47]. We selected our threshold for visual clarity of known anatomical structures. The influence of the binarization threshold on the resulting bundlings is shown in Fig. 6. After binarization, short edges (<20 mm) were removed, resulting in 6,630 connections (Fig. 1).

To examine the sensitivity of the method to different data sets, we also randomly picked 20 single data sets and 20 groups of 20 subjects each (Figs. S1-S4, which can be found on the Computer Society Digital Library at http://doi.ieeecomputersociety.org/10.1109/TVCG.2013.114). To further show the transferability of the method, we derived and spatially aligned an independent connectivity graph from a DWI example data set (Fig. 5 and S6, available in the online supplemental material).

The *detail data set* from a healthy participant was acquired and preprocessed as previously described [48]. To show the detail inherent in connectivity, two ROIs were manually defined in the left frontal and temporal lobe after extracting the surface of the cortex. Only connections between these ROIs were thresholded ($z > 0.35$), and short edges (<20 mm) were removed to create a second binary graph consisting of 7,799 edges (Fig. 2).

3.2 Algorithm

Our bundling algorithm combines steps from FDEB [36] and KDEEB [37]. We first calculate a measure of similarity between edges, which guarantees that only *compatible* edges are bundled together. We then iteratively subdivide the edges, and move subdivision points to areas with higher density.

3.2.1 Compatibility

We use the definition of pairwise similarity between edges from FDEB. *Compatibility* is defined as a product of four geometrical criteria: similarities of angle and length, distance between midpoints, and the visibility. These criteria are mapped to ranges between 1 for identical edges, and 0 for dissimilar edges. We refer to the original paper for the details [36].

3.2.2 Iteration and Subdivision Scheme

We iteratively subdivide the edges. Similar to FDEB, we use a scheme of k cycles consisting of i iterations. Between cycles, we subdivide the edges by insertion of subdivision points p_1 to p_n at regular intervals. FDEB doubles the number of line segments with each cycle. We chose to use a noninteger factor for the increase of subdivision points per cycle, such as in the implementation of FDEB available in JFlowMap.[3] We set the number of segments to 1.3^c, with c being the number of the current cycle. Compared with doubling, this results in a slower growth of the number of subdivision points. In addition, the connections are smoothed between cycles, since new subdivision points are created between the subdivision points from the old cycle. We found that a linear reduction of iterations over cycles leads to good results. Our iteration scheme consists of 10 cycles, starting with 10 iterations, and ending with one.

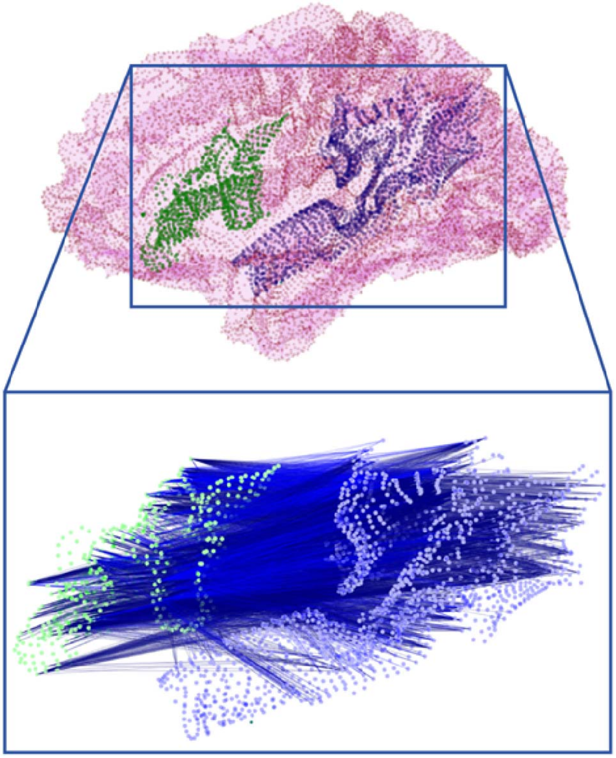

Fig. 2. Detail data of connectivity between 1,000 nodes in two ROIs (in green and blue) in left-lateral prefrontal and temporal areas in a single brain, which are, among others, involved in language processing and production. As in Fig. 1, in the unbundled graph the structure is not apparent before our application of edge bundling.

3.2.3 Mean-Shift of Subdivision Points

To calculate the new position for each subdivision point in each iteration, we use a method similar to mean-shift clustering [49], a nonparametric method that does not require the explicit number of clusters as input. We move each point to a weighted mean of all *compatible* surrounding control points. As in FDEB, we consider subdivision points compatible if they occupy the same position along the edges and the compatibility between the edges is above a user-defined threshold c_{thr}.

The weights for the calculation of the new position are determined using a Gaussian kernel $K(d) = e^{-d^2 / 2\sigma^2}$ on the distance d between subdivision points. The width of the Gaussian kernel σ, and the aforementioned compatibility threshold c_{thr} influence the results globally. c_{thr} also influences how many distinct bundles emerge. Similarly, σ influences whether the bundling is coarser or more fine

---

[3] http://code.google.com/p/jflowmap.

grained. To determine optimal parameters, we calculated solutions for different compatibility thresholds and Gaussian kernel widths (see Fig. S5, available in the online supplemental material). We picked a solution that was not underbundled or overbundled by visual inspection of all results. Although the decision of optimal parameters remains subjective, we based it on clarity of the known connectomic structures. The result of changing the parameters is predictable: changing the compatibility threshold influences the number of distinct bundles, while changing the kernel width influences the curvature of the resulting bundles. Although both parameters also influence each other, this makes it possible to iteratively refine a result until the desired granularity and appearance are reached. We heuristically determined the following parameters for our visualizations: $c_{thr} = 0.8$ for the detail data set, and 0.7 for the whole-brain data set, and $\sigma = 5$ mm for both data sets.

3.2.4 Bundle Clustering

The mean-shift method is generally used for clustering, and in our case moves compatible groups of subdivision points toward their common center of gravity. Since the points in the middle of the connections are moved through more iterations compared with the ones closer to the termination points, these parts of the edges are pulled together especially close, which forms the connections into distinct bundles. We can then use the distance of the connections after bundling to algorithmically determine subdivisions in order to colorize individual bundles differently.

Individual bundles are determined by iterating through the connections, and assigning them to a new bundle if they are not closer than a small radius $r = 0.5$ mm to a connection that is already assigned, and to the bundle containing the closest assigned connection otherwise.

3.2.5 Implementation and Efficiency

We implemented the algorithm in C++, and make our source code available on GitHub[4] and on Google Code.[5] The calculation of the two examples takes 16 and 8 s, for the whole-brain and the detail data set, respectively. Note that the more complex data set takes less time to compute, since the higher c_{thr} reduces the number of required interactions between edges. The computations were performed on an 8-core CPU with 3.4 GHz.

3.2.6 Rendering

For the visualization of the resulting connectivity bundles in connection with anatomical surface features, we believe transparent rendering, high-quality lighting, shadow, and depth cues play an important role. For our renderings of the results of the bundling process in connection with the anatomy of the brain, we exported cortical surfaces derived with FreeSurfer—a software designed to perform extraction of this surface from MRI data [50]—and the edge bundles to Cinema 4D, a cinematic rendering software package (MAXON Computer GmbH).

3.3 Results

The result of our method are spline-like bundles of similar connections that avoid clutter by sharing screen-space in their middle section and take up less overall space than the straight lines. In the context of visualizing brain connectivity, our method has the advantage that the shape of the resulting bundles is independent from the density of connections in different parts of the space (Fig. 3).

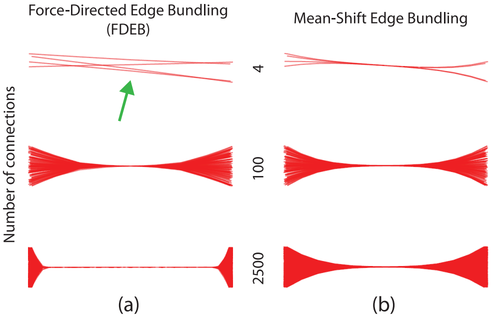

Fig. 3. This artificial example shows the difference of force-directed edge bundling and our method in the application to bundles with different densities. FDEB (a) bundles denser sets faster than bundles containing only few connections. This leaves the latter underbundled in comparison with the denser bundles (green arrow). Our algorithm bundles all densities evenly (b).

Functional connectivity data consist of heterogeneous groups of connections between brain areas with different sizes. Therefore, some of the resulting bundles consist only of a few edges, while others consist of hundreds or thousands. We found that with the original simulation of electrostatic forces the large bundles tend to get bundled too quickly, while smaller bundles remain loose. The impact of FDEB on an artificial example of two bundles with extremely different density is shown in Fig. 3a. The problem is compounded by the extreme differences in bundle size in brain data, and the fact that the bundles also influence each other.

The effect of our method is that bundles with different density converge evenly, and without the numerical issues that arise from the simulation of physical forces in FDEB. The result of the application of our adapted method is shown in Fig. 3b. KDEEB has a similar independence from the bundle density, but the calculation of a global density field for all subdivision points prohibits the incorporation of a pairwise compatibility measure, which we found necessary to avoid unsatisfactory bundlings in three dimensions.

In the group data (Fig. 4), our method shows networks of long-range connectivity that are well established in the neuroimaging literature (for example, [51]). These include the default-mode network, as well as visual, sensorimotor, and the dorsal fronto-parietal networks. The most obvious feature in the visualizations is the wide-scale lateral symmetry in the connections between the two hemispheres, especially in the sensorimotor system.

That our bundling method is stable with regard to the application to different data sets is shown by the high similarity between the bundlings of the group data and the randomly selected individual data sets and subgroups (Figs. S1-S4, available in the online supplemental material). Even for an independent data set with connectivity derived from DWI data, bundling with identical parameters yields a satisfying result (Fig. 5 and S6, available in the online supplemental material).

There is substantial precedence in the literature on anotomical and functional connectivity to account for the

---

[4] https://github.com/NeuroanatomyAndConnectivity/brainbundler.
[5] http://code.google.com/p/braingl/.

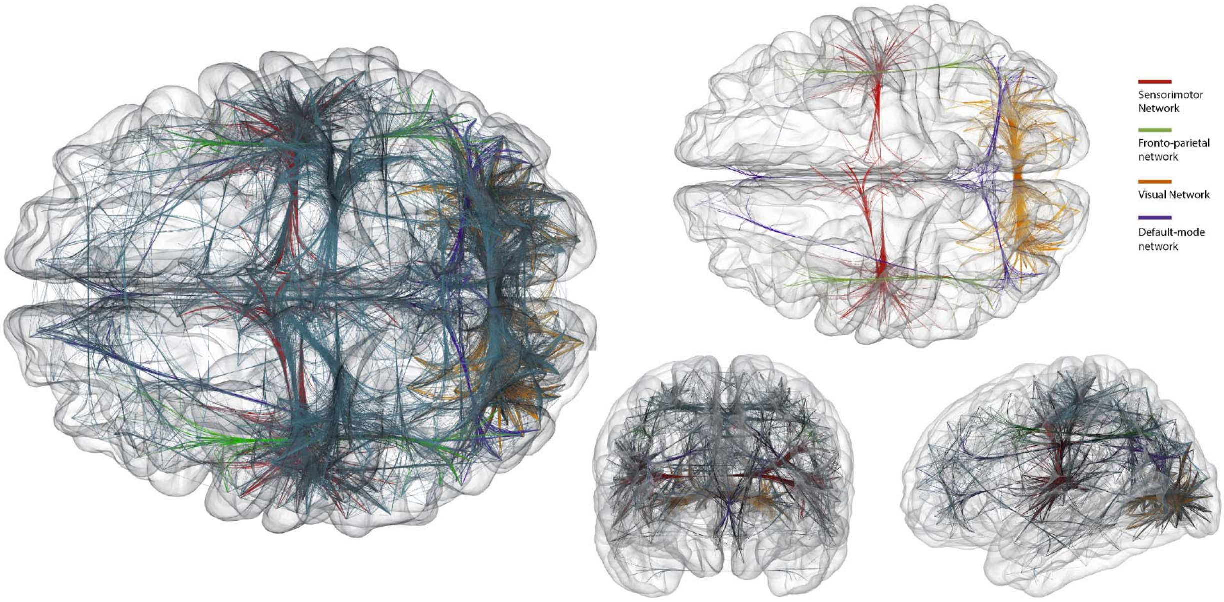

Fig. 4. Whole-brain group-level connectivity. While in the unbundled graph, nearly no structure is visible (see Fig. 1d), our visualization clarifies several well-known functional networks, wide-scale lateral symmetry of brain organization, as well as fine details in functional organization. The four labeled networks (top right) were manually selected and colored to illustrate their embedding in the overall visualization.

differences observed between the two sets of bundling results. One reason for the lack of a one-to-one correspondence between anatomical and functional connectivity lies in indirect functional connections between areas, thus demonstrating functional connectivity in the absence of a direct anatomical connection [5]. In addition, the dynamics of functional connectivity indicate that they may be guided by anatomical connections, but not determined by them [52].

Robustness with regard to the binarization threshold and the associated change in the number of edges can be seen in Fig. 6. These results support the possibility of using our method for a wide range of brain data without requiring drastic changes to the parameters.

In the detail data set (Fig. 7), the visualization is able to clearly show that the chosen frontal and temporal areas consist of several interconnected centers. These areas on the left hemisphere are among others associated with language processing and production [28], [57]. For the latter example, the data were subdivided into 17 distinct bundles by the procedure described in Section 3.2. We colored the bundles with arbitrarily chosen distinct colors, which help to determine the connections between the different centers by facilitating the visual differentiation of independent clusters of connections (Fig. 7).

4 CONCLUSION

We have presented here the first application of an edge bundling technique to functional connectivity graphs in native three-dimensional brain space. The result of our technique, which is based on FDEB and KDEEB, is visualizations that are able to show full graphs of functional connectivity as well as fine details in high-resolution single-brain data.

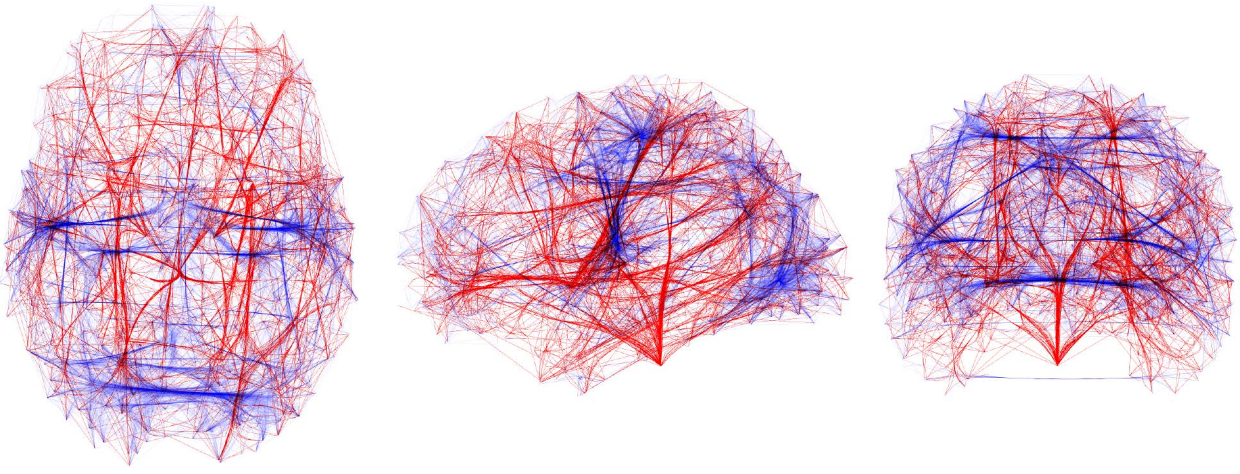

Fig. 5. Comparison between functional (blue) and anatomical (red) connectivity. The anatomical connectivity data are a binary graph derived from DWI data using probabilistic fiber tracking. We bundled both data sets with the same parameters ($c_{thr} = 0.7$, $\sigma = 5$ mm). Both bundlings do not necessarily follow anatomical fiber tracts, but are abstract visualizations of connectivity in anatomical space.

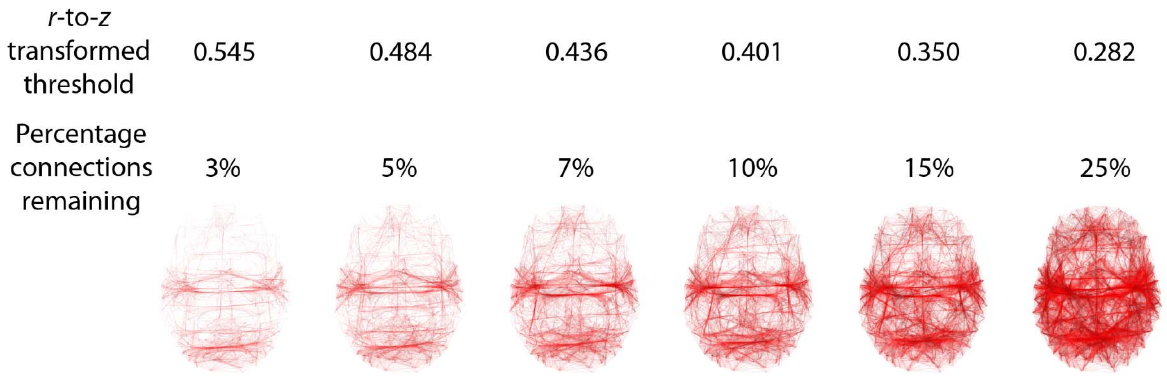

Fig. 6. Influence of binarization threshold on the bundling results using the functional connectivity whole-brain group-level data. Identical values are used for the compatibility threshold and Gaussian kernel width ($c_{thr} = 0.7$, $\sigma = 5$ mm). The structure of the bundlings remains similar.

Although for an overview of global connectivity patterns and their changes, more abstract layouts might be more appropriate, the anatomical faithfulness of our method makes it a valuable tool in the exploration of the human connectome, for example, for illustrating results from statistical comparisons of connectivity differences between groups. Due to the same property, the application to clinical contexts, especially neurosurgery, is also promising, offering a quick overview of distorted connectivity patterns. From a practical standpoint, resting-state fMRI has numerous advantages over task-based approaches for clinical application [20], [53], [54], mainly due to its short acquisition time and post hoc versatility. The method could be especially helpful for presurgical planning prior to tumor resections. Information about the localization of functional areas in relation to a lesion can potentially influence the decision to intervene, the surgical approach, and the degree of resection; resolution, neighborhood, and distance relations are essential for such applications.

Edge bundling may also provide a valuable modeling tool for the development of white matter tracts in conjunction with morphometric constraints. A comparison of the results from edge bundling and the anatomical shape of the white matter tracts is promising (Fig. 5 and S6, available in the online supplemental material). In the future, inclusion of anatomical constraints (interhemispheric fibers have to pass through the corpus callosum, etc.) may bring us closer to a simulation of white matter fiber behavior and, therefore, inform us about their organization. It is important to keep in mind that we visualize abstract functional connectivity information, which is related to, but does not necessarily coincide with the underlying anatomical connections. For the aforementioned applications, however, the correspondence with the anatomical space is crucial. Calamante et al. [31] (see Section 2.2.2) have proven that combining the two connectivity modalities can yield informative and aesthetically impressive renderings of functionally informed anatomy. A similar combination of edge bundling with anatomical connectivity data could also lead to highly informative

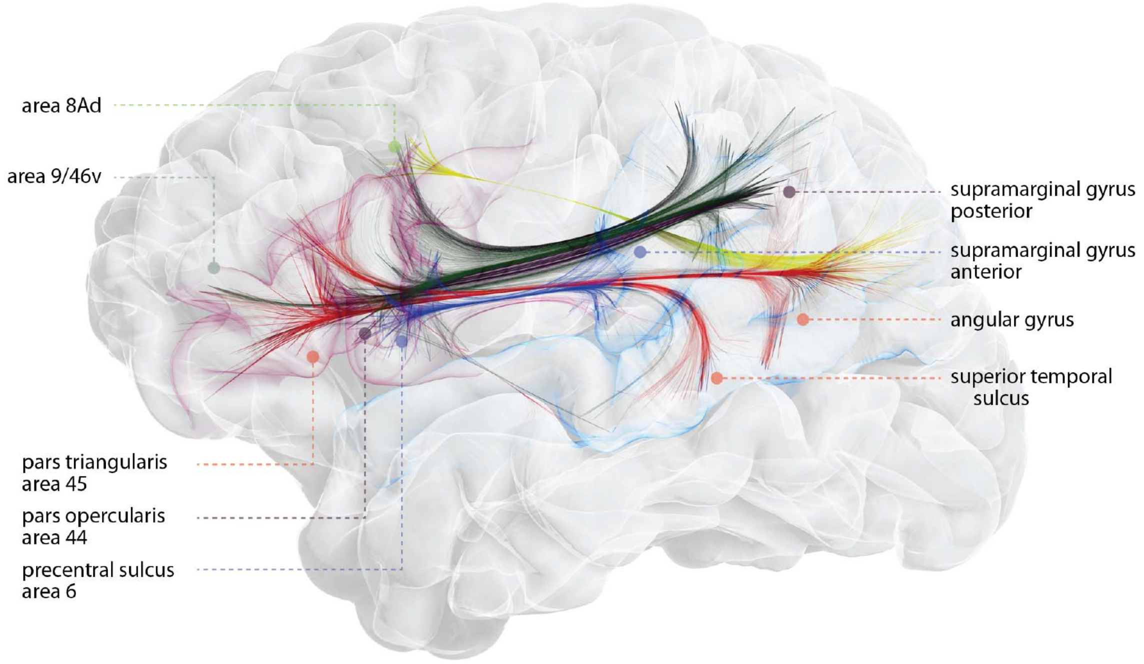

Fig. 7. Single-case connectivity detail: While the unbundled graph (see Fig. 2) makes it hard to discern any structure, bundling reveals several functionally connected areas. The colorization of the distinct bundles is the result of our bundle clustering technique described in Section 3.2.

visualizations. However, our method currently facilitates the visualization of functional connectivity independently from DWI data. We believe the differences between functional and anatomical connectivity patterns presented in Fig. 5 further underline the caution that should be taken in attempting to superficially drive the results of one form of connectivity using the other.

Exploratory connectivity visualization may benefit from following even more radically different paths than nature. Mapping anatomy and connections to topology-preserving partially or fully inflated brains, or flatmaps [55], as well as forcing connections to run outside of the cortical surface in the manner of annotations, may facilitate visual comprehension, while also informing about underlying organization (for example, see [56, Fig. 5]).

As Dixhoorn et al. [21] have pointed out, the problem of the visualization of functional connectivity is located at the nexus of scientific and information visualization. They consequentially adapted techniques from visual analytics, such as multiple coupled anatomical and abstract views to aid the iterative exploratory selection of interesting aspects from a full data set. Similar methods are frequently used in the analysis of DWI data, and we plan to incorporate them in future development of interactive software.

Visual analytics strives to incorporate a back and forth between visualization and analytic techniques. We believe the distinction between methods to computationally extract information, and the methods to visualize it, is often arbitrary, and an integrated solution is necessary to make exploration of the data successful. Edge bundling offers a method from the visualization community to help clarify the combined complexity of integrating graph information with three-dimensional space—a problem at the heart of understanding the brain. Future elaboration of these approaches will no doubt facilitate research into the intricate organization of neural connections.

ACKNOWLEDGMENTS

The authors would like to thank Tobias S. Hoffmann for expert assistance with the rendering of the visualizations, Krzysztof J. Gorgolewski for his helpful comments on the manuscript, and the members of the Neuro Bureau for continued creative input. This work was made possible through support from the Max Planck Society.

REFERENCES

[1] K.J. Friston, C.D. Frith, P.F. Liddle, and R.S. Frackowiak, “Functional Connectivity: The Principal-Component Analysis of Large (Pet) Data Sets,” *J. Cerebral Blood Flow and Metabolism,* vol. 13, no. 1, pp. 5-14, 1993.

[2] B. Biswal, F.Z. Yetkin, V.M. Haughton, and J.S. Hyde, “Functional Connectivity in the Motor Cortex of Resting Human Brain Using Echo-Planar MRI,” *Magnetic Resonance Medicine,* vol. 34, no. 4, pp. 537-541, 1995.

[3] M.D. Fox and M.E. Raichle, “Spontaneous Fluctuations in Brain Activity Observed with Functional Magnetic Resonance Imaging,” *Nature Rev. Neuroscience,* vol. 8, no. 9, pp. 700-711, 2007.

[4] F. Crick and E. Jones, “Backwardness of Human Neuroanatomy,” *Nature,* vol. 361, no. 6408, pp. 109-110, 1993.

[5] M.P. van den Heuvel, R.C.W. Mandl, R.S. Kahn, and H.E. Hulshoff Pol, “Functionally Linked Resting-State Networks Reflect the Underlying Structural Connectivity Architecture of the Human Brain,” *Human Brain Mapping,* vol. 30, no. 10, pp. 3127-3141, 2009.

[6] Y. Masutani, S. Aoki, O. Abe, N. Hayashi, and K. Otomo, “MR Diffusion Tensor Imaging: Recent Advance and New Techniques for Diffusion Tensor Visualization,” *European J. Radiology,* vol. 46, no. 1, pp. 53-66, 2003.

[7] S. Pajevic and C. Pierpaoli, “Color Schemes to Represent the Orientation of Anisotropic Tissues from Diffusion Tensor Data: Application to White Matter Fiber Tract Mapping in the Human Brain,” *Magnetic Resonance Medicine,* vol. 42, no. 3, pp. 526-540, 1999.

[8] T. Schultz and G.L. Kindlmann, “Superquadric Glyphs for Symmetric Second-Order Tensors,” *IEEE Trans. Visualization and Computer Graphics,* vol. 16, no. 6, pp. 1595-1604, Nov./Dec. 2010.

[9] T.E. Conturo, N.F. Lori, T.S. Cull, E. Akbudak, A.Z. Snyder, J.S. Shimony, R.C. McKinstry, H. Burton, and M.E. Raichle, “Tracking Neuronal Fiber Pathways in the Living Human Brain,” *Proc. Nat’l Academy of Sciences of USA,* vol. 96, no. 18, pp. 10422-10427, 1999.

[10] S. Mori, B.J. Crain, V.P. Chacko, and P.C. van Zijl, “Three-Dimensional Tracking of Axonal Projections in the Brain by Magnetic Resonance Imaging,” *Ann. Neurology,* vol. 45, no. 2, pp. 265-269, 1999.

[11] V. Wedeen, “Diffusion Aniostropy and White Matter Tracts,” *Proc. Second Int’l Conf. Functional Mapping of the Human Brain,* 1996.

[12] R. Jianu, C. Demiralp, and D.H. Laidlaw, “Exploring Brain Connectivity with Two-Dimensional Neural Maps,” *IEEE Trans. Visualization & Computer Graphics,* vol. 18, no. 6, pp. 978-987, June 2012.

[13] M.H. Everts, H. Bekker, J.B.T.M. Roerdink, and T. Isenberg, “Depth-Dependent Halos: Illustrative Rendering of Dense Line Data,” *IEEE Trans. Visualization & Computer Graphics,* vol. 15, no. 6, pp. 1299-1306, Nov./Dec. 2009.

[14] T. Schultz, H. Theisel, and H.-P. Seidel, “Topological Visualization of Brain Diffusion MRI Data,” *IEEE Trans. Visualization & Computer Graphics,* vol. 13, no. 6, pp. 1496-1503, Nov./Dec. 2007.

[15] A. Berres, M. Goldau, M. Tittgemeyer, G. Scheuermann, and H. Hagen, “Tractography in Context: Multimodal Visualization of Probabilistic Tractograms in Anatomical Context,” *Proc. Eurographics Workshop Visual Computing for Biology and Medicine,* pp. 9-16, 2012.

[16] A. von Kapri, T. Rick, S. Caspers, S.B. Eickhoff, K. Zilles, and T. Kuhlen, “Evaluating a Visualization of Uncertainty in Probabilistic Tractography,” *Proc. SPIE,* vol. 7625, 2010.

[17] D.S. Margulies, J. Bottger, A. Watanabe, and K.J. Gorgolewski, “Visualizing the Human Connectome,” *NeuroImage,* vol. 80, pp. 445-461, 2013.

[18] Z.S. Saad and R.C. Reynolds, “Suma,” *NeuroImage,* vol. 62, no. 2, pp. 768-773, 2012.

[19] R.W. Cox, “AFNI: Software for Analysis and Visualization of Functional Magnetic Resonance Neuroimages,” *Computers and Biomedical Research,* vol. 29, no. 3, pp. 162-173, 1996.

[20] J. Böttger, D.S. Margulies, P. Horn, U.W. Thomale, I. Podlipsky, I. Shapira-Lichter, S.J. Chaudhry, C. Szkudlarek, K. Mueller, G. Lohmann, T. Hendler, G. Bohner, J.B. Fiebach, A. Villringer, P. Vajkoczy, and A. Abbushi, “A Software Tool for Interactive Exploration of Intrinsic Functional Connectivity Opens New Perspectives for Brain Surgery,” *Acta Neurochirurgica (Wien),* vol. 153, no. 8, pp. 1561-1572, 2011.

[21] A. van Dixhoorn, B. Vissers, L. Ferrarini, J. Milles, and C.P. Botha, “Visual Analysis of Integrated Resting State Functional Brain Connectivity and Anatomy,” *Proc. Eurographics Workshop Visual Computing for Biology and Medicine,* pp. 57-64, 2010.

[22] D.S. Margulies, J. Bottger, X. Long, Y. Lv, C. Kelly, A. Schafer, D. Goldhahn, A. Abbushi, M.P. Milham, G. Lohmann, and A. Villringer, “Resting Developments: A Review of fMRI Post-Processing Methodologies for Spontaneous Brain Activity,” *MAGMA,* vol. 23, nos. 5/6, pp. 289-307, 2010.

[23] K.J. Worsley, J.-I. Chen, J. Lerch, and A.C. Evans, “Comparing Functional Connectivity via Thresholding Correlations and Singular Value Decomposition,” *Philosophical Trans. Royal Soc. London Series B, Biological Sciences,* vol. 360, no. 1457, pp. 913-920, 2005.

[24] S. Mikula and E. Niebur, “A Novel Method for Visualizing Functional Connectivity Using Principal Component Analysis,” *Int’l J. Neuroscience,* vol. 116, no. 4, pp. 419-429, 2006.

[25] R. Salvador, J. Suckling, M.R. Coleman, J.D. Pickard, D. Menon, and E. Bullmore, “Neurophysiological Architecture of Functional

Magnetic Resonance Images of Human Brain," *Cerebral Cortex,* vol. 15, no. 9, pp. 1332-1342, 2005.

[26] S. Achard, R. Salvador, B. Whitcher, J. Suckling, and E. Bullmore, "A Resilient, Low-Frequency, Small-World Human Brain Functional Network with Highly Connected Association Cortical Hubs," *J. Neuroscience,* vol. 26, no. 1, pp. 63-72, 2006.

[27] D.S. Margulies, J.L. Vincent, C. Kelly, G. Lohmann, L.Q. Uddin, B.B. Biswal, A. Villringer, F.X. Castellanos, M.P. Milham, and M. Petrides, "Precuneus Shares Intrinsic Functional Architecture in Humans and Monkeys," *Proc. Nat'l Academy of Sciences of USA,* vol. 106, no. 47, pp. 20069-20074, 2009.

[28] C. Kelly, L.Q. Uddin, Z. Shehzad, D.S. Margulies, F.X. Castellanos, M.P. Milham, and M. Petrides, "Broca's Region: Linking Human Brain Functional Connectivity Data and Non-Human Primate Tracing Anatomy Studies," *European J. Neuroscience,* vol. 32, no. 3, pp. 383-398, 2010.

[29] M.D. Greicius, K. Supekar, V. Menon, and R.F. Dougherty, "Resting-State Functional Connectivity Reflects Structural Connectivity in the Default Mode Network," *Cerebral Cortex,* vol. 19, no. 1, pp. 72-78, 2009.

[30] T.E. Behrens and O. Sporns, "Human Connectomics," *Current Opinion in Neurobiology,* vol. 22, no. 1, pp. 144-153, 2012.

[31] F. Calamante, R.A.J. Masterton, J.-D. Tournier, R.E. Smith, L. Willats, D. Raffelt, and A. Connelly, "Track-Weighted Functional Connectivity (TW-FC): A Tool for Characterizing the Structural-Functional Connections in the Brain," *NeuroImage,* vol. 70, pp. 199-210, 2013.

[32] D. Holten, "Hierarchical Edge Bundles: Visualization of Adjacency Relations in Hierarchical Data," *IEEE Trans. Visualization & Computer Graphics,* vol. 12, no. 5, pp. 741-748, Sep./Oct. 2006.

[33] J. McGonigle, A.L. Malizia, and M. Mirmehdi, "Visualizing Functional Connectivity in fMRI Using Hierarchical Edge Bundles," *Proc. Abstract and Poster Presented at the 17th Ann. Meeting of the Organization for Human Brain Mapping,* 2011.

[34] A. Irimia, M.C. Chambers, C.M. Torgerson, and J.D.V. Horn, "Circular Representation of Human Cortical Networks for Subject and Population-Level Connectomic Visualization," *NeuroImage,* vol. 60, no. 2, pp. 1340-1351, 2012.

[35] M. Balzer and O. Deussen, "Level-of-Detail Visualization of Clustered Graph Layouts," *Proc. Sixth Int'l Asia-Pacific Symp. Visualisation (APVIS '07),* 2007.

[36] D. Holten and J.J. van Wijk, "Force-Directed Edge Bundling for Graph Visualization," *Computer Graphics Forum,* vol. 28, no. 3, pp. 983-990, 2009.

[37] C. Hurter, O. Ersoy, and A. Telea, "Graph Bundling by Kernel Density Estimation," *Computer Graphics Forum,* vol. 31, no. 3, pp. 865-874, 2012.

[38] E.R. Gansner, H. Yifan, S. North, and C. Scheidegger, "Multilevel Agglomerative Edge Bundling for Visualizing Large Graphs," *Proc. IEEE Pacific Visualization Symp. (PacificVis),* pp. 187-194. 2011.

[39] A. Lambert, R. Bourqui, and D. Auber, "3D Edge Bundling for Geographical Data Visualization," *Proc. 14th Int'l Conf. Information Visualisation (IV),* pp. 329-335, 2010.

[40] W. Cui, H. Zhou, H. Qu, P.C. Wong, and X. Li, "Geometry-Based Edge Clustering for Graph Visualization," *IEEE Trans. Visualization & Computer Graphics,* vol. 14, no. 6, pp. 1277-1284, Nov./Dec. 2008.

[41] O. Ersoy, C. Hurter, F.V. Paulovich, G. Cantareira, and A. Telea, "Skeleton-Based Edge Bundling for Graph Visualization," *IEEE Trans. Visualization & Computer Graphics,* vol. 17, no. 12, pp. 2364-2373, Dec. 2011.

[42] A. Telea and O. Ersoy, "Image-Based Edge Bundles: Simplified Visualization of Large Graphs," *Computer Graphics Forum,* vol. 29, no. 3, pp. 843-852, 2010.

[43] B.B. Biswal, M. Mennes, X.-N. Zuo, S. Gohel, C. Kelly, S.M. Smith, C.F. Beckmann, J.S. Adelstein, R.L. Buckner, S. Colcombe, A.-M. Dogonowski, M. Ernst, D. Fair, M. Hampson, M.J. Hoptman, J.S. Hyde, V.J. Kiviniemi, R. Kötter, S.-J. Li, C.-P. Lin, M.J. Lowe, C. Mackay, D.J. Madden, K.H. Madsen, D.S. Margulies, H.S. Mayberg, K. McMahon, C.S. Monk, S.H. Mostofsky, B.J. Nagel, J.J. Pekar, S.J. Peltier, S.E. Petersen, V. Riedl, S.A.R.B. Rombouts, B. Rypma, B.L. Schlaggar, S. Schmidt, R.D. Seidler, G.J. Siegle, C. Sorg, G.-J. Teng, J. Veijola, A. Villringer, M. Walter, L. Wang, X.-C. Weng, S. Whitfield-Gabrieli, P. Williamson, C. Windischberger, Y.-F. Zang, H.-Y. Zhang, F.X. Castellanos, and M.P. Milham, "Toward Discovery Science of Human Brain Function," *Proc. Nat'l Academy of Sciences of USA,* vol. 107, no. 10, pp. 4734-4739, 2010.

[44] M.P. Milham, "Open Neuroscience Solutions for the Connectome-Wide Association Era," *Neuron,* vol. 73, no. 2, pp. 214-218, 2012.

[45] L. Cammoun, X. Gigandet, D. Meskaldji, J.P. Thiran, O. Sporns, K.Q. Do, P. Maeder, R. Meuli, and P. Hagmann, "Mapping the Human Connectome at Multiple Scales with Diffusion Spectrum MRI," *J. Neuroscience Methods,* vol. 203, no. 2, pp. 386-397, 2012.

[46] M.D. Fox, D. Zhang, A.Z. Snyder, and M.E. Raichle, "The Global Signal and Observed Anticorrelated Resting State Brain Networks," *J. Neurophysiology,* vol. 101, no. 6, pp. 3270-3283, 2009.

[47] K. Murphy, R.M. Birn, D.A. Handwerker, T.B. Jones, and P.A. Bandettini, "The Impact of Global Signal Regression on Resting State Correlations: Are Anti-Correlated Networks Introduced?" *NeuroImage,* vol. 44, no. 3, pp. 893-905, 2009.

[48] M. Taubert, G. Lohmann, D.S. Margulies, A. Villringer, and P. Ragert, "Long-Term Effects of Motor Training on Resting-State Networks and Underlying Brain Structure," *NeuroImage,* vol. 57, no. 4, pp. 1492-1498, 2011.

[49] K. Fukunaga and L.D. Hostetler, "Estimation of Gradient of a Density-Function, with Applications in Pattern-Recognition," *IEEE Trans. Information Theory,* vol. IT-21, no. 1, pp. 32-40, Jan. 1975.

[50] A.M. Dale, B. Fischl, and M.I. Sereno, "Cortical Surface-Based Analysis. I. Segmentation and Surface Reconstruction," *NeuroImage,* vol. 9, no. 2, pp. 179-194, 1999.

[51] S.M. Smith, P.T. Fox, K.L. Miller, D.C. Glahn, P.M. Fox, C.E. Mackay, N. Filippini, K.E. Watkins, R. Toro, A.R. Laird, and C.F. Beckmann, "Correspondence of the Brain's Functional Architecture during Activation and Rest," *Proc. Nat'l Academy of Sciences of USA,* vol. 106, no. 31, pp. 13040-13045, 2009.

[52] R.L. Buckner, F.M. Krienen, and B.T.T. Yeo, "Opportunities and Limitations of Intrinsic Functional Connectivity MRI," *Nature Neuroscience,* vol. 16, no. 7, pp. 832-837, June 2013.

[53] J.S. Shimony, D. Zhang, J.M. Johnston, M.D. Fox, A. Roy, and E.C. Leuthardt, "Resting-State Spontaneous Fluctuations in Brain Activity: A New Paradigm for Presurgical Planning Using fMRI," *Academic Radiology,* vol. 16, no. 5, pp. 578-583, 2009.

[54] D. Zhang, J.M. Johnston, M.D. Fox, E.C. Leuthardt, R.L. Grubb, M.R. Chicoine, M.D. Smyth, A.Z. Snyder, M.E. Raichle, and J.S. Shimony, "Preoperative Sensorimotor Mapping in Brain Tumor Patients Using Spontaneous Fluctuations in Neuronal Activity Imaged with Functional Magnetic Resonance Imaging: Initial Experience," *Neurosurgery,* vol. 65, suppl. no. 6, pp. 226-236, 2009.

[55] B. Fischl, M.I. Sereno, and A.M. Dale, "Cortical Surface-Based Analysis. II: Inflation, Flattening, and a Surface-Based Coordinate System," *NeuroImage,* vol. 9, no. 2, pp. 195-207, 1999.

[56] J.R. Foucher, P. Vidailhet, S. Chanraud, D. Gounot, D. Grucker, D. Pins, C. Damsa, and J.-M. Danion, "Functional Integration in Schizophrenia: Too Little or Too Much? Preliminary Results on fMRI Data," *NeuroImage,* vol. 26, no. 2, pp. 374-388, 2005.

[57] D.S. Margulies and M. Petrides, "Distinct Parietal and Temporal Connectivity Profiles of Ventrolateral Frontal Areas Involved in Language Production," *J. Neuroscience,* vol. 33, no. 42, pp. 16846-16852, 2013.

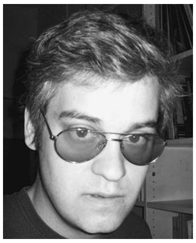

Joachim Böttger received the diploma in computational visualistics from Magdeburg University, in 2003, and a doctorate in computer science from the University of Konstanz, in 2009. He was a research scientist in the Department for Neurosurgery of Charité - University Medicine Berlin, and is currently a researcher at the Max Planck Institute for Human Brain and Cognitive Sciences in Leipzig; he has authored or coauthored 11 scientific papers. His current research interests include the visualization of functional connectivity and its clinical application.

Alexander Schäfer received the diploma in computer science in 2009, and is currently working toward a doctoral degree at the Max Planck Institute for Human Brain and Cognitive Sciences in Leipzig. His research interests include the application of graph-theory to neuroscience.

Gabriele Lohmann received the diploma in mathematics in 1984, and a doctorate in computer science in 1991. She is currently a senior researcher at the Max Planck Institute for Human Brain and Cognitive Sciences in Leipzig where she develops new analysis methods for imaging data.

Arno Villringer received an MD degree from Freiburg University in 1984, and trained in neurology at the University of Munich (1986-1992). He is currently the director of the Max Planck Institute for Human Brain and Cognitive Sciences in Leipzig, the director of the clinic for cognitive neurology at the University Hospital, Leipzig, a coordinator of the German competence net stroke, and a speaker of the Berlin School of Mind and Brain. His research interest focuses on stroke.

Daniel S. Margulies received a doctorate for his research on applications of resting-state functional connectivity to the study of neuroanatomy, for which he received the Otto Hahn Medal in 2010. He is currently the group leader of the Max Planck Research Group: Neuroanatomy & Connectivity in Leipzig.